Department of the Navy
Office of Naval Research
Contract N6onr-24420 (NR 062-059)
Contract N6onr-24435 (NR 062-124)

SCALE EFFECTS IN CAVITATING FLOW

Blaine R. Parkin

Hydrodynamics Laboratory
California Institute of Technology
Pasadena, California

Report No. 21-8
July 31, 1952

Approved by:
M. S. Plesset

CONTENTS

ABSTRACT

Scale effects in cavitating flow are considered for the so-called limited cavitation flow regime. The effects on cavitation scaling of nuclei and dissolved air in ordinary water are considered. Previous work by the author is summarized and a theoretical study is made to gain insight into the relationships that must hold between the parameters which affect the inception of cavitation. A simplified theory gives only rough qualitative agreement with experiment.

PART I

INITIAL CONSIDERATIONS

Introduction

The present work is a sequel to the author's preliminary report[1]* on the effects of body size and free stream velocity upon cavitation on an immersed body. The nomenclature of this report will follow that used in the preliminary paper.

It is useful to divide the flow of a liquid around a solid body into three regimes[1] which are called noncavitating flow, limited cavitation, and full cavity flow, respectively. The scaling laws which control the behavior of flows in the noncavitating regime have been well known for some time. For full cavity flows, Reichardt[2] has shown that the essential quantity for determining the flow geometry is the cavitation number, $K = (p_o - p_v)/\frac{1}{2}\rho V_o^2$, where p_o and V_o are the free stream values of the static pressure and velocity, respectively, and ρ is the liquid density. Reichardt takes for p_v the sum of all gas pressures within the cavity. In the present work, p_v will denote only the liquid vapor pressure. However, for the limited cavitation flow regime there is a definite lack of knowledge concerning the effects of body size, flow velocity, and dissolved air content upon the development of cavitation. In fact, it is now customary to employ the cavitation number K as the only significant parameter for describing all inviscid cavitating flows. It is shown in this paper by both theoretical and experimental means that the use of

---

*See bibliography on page 38.

only the cavitation number for limited cavitation is an unjustified simplification.

The object of this study is to determine the behavior of limited cavitation on a given body shape placed in a rectilinear flow of constant free stream velocity. Such a flow is approximated in the test section of a water tunnel where the free stream velocity, free stream static pressure, and the amount of air dissolved in the water can be controlled as required. If one considers only this elementary flow configuration, very simple experiments* can be performed. For such experiments, the spatial pressure distributions on the body surface will be known. From these known pressure distributions and the free stream velocity, pressure-time relationships can be calculated for a particle moving along the body surface with the liquid. From such pressure-time functions, one can study analytically the behavior of incipient cavitation with changing body scales. In this report such calculations are made and compared with experiment.

Possible Origin of Cavitation

For ordinary untreated water it will be assumed that there are nuclei containing air or water vapor, or both, which are stabilized on small, solid particles in the liquid. It is held that boiling or cavitation must be initiated from such nuclei, since their absence would mean that very large surface tension forces must be overcome before cavitation can start. The slight tension under which cavitation normally occurs lends plausibility to arguments favoring the existence of the nuclei. If one supposes that cavitation originates from such small nuclei, then it must take them an appreciable time to grow to a macroscopic size. It is clear that this growth time must be dependent upon the pressure to which the nuclei are subjected. If for a constant free stream pressure and velocity only the scale of the immersed body is changed, the liquid flow may show corresponding changes in the cavitation due to changes in the time available for bubble growth. Under steady, or almost steady, conditions, ordinary untreated water has a definite boiling point and has no appreciable tensile strength. Such water will, however, withstand tensions if it is subjected to transient low pressures of short duration. For water flowing around a solid body, such short duration transient tensions can be produced on the water as it flows

*The experiments performed for this study are described in Ref. 1.

by the body surface. It is possible that the differences in the transient tensions produced by changes in body length and free stream velocity can account for corresponding differences in the state of cavitation. It is the study of nucleus response under these transient pressure conditions that is of primary concern here.

Summary of Previous Results

In the preliminary report, the assumption that cavitation starts from small nuclei in the liquid gives conditions for dynamically similar bubble growths. It was found that no useful scaling laws for limited cavitation can be obtained from such similarity arguments. In fact, the similarity calculations indicated that the cavitation number, K, is not the significant parameter for defining the state of the flow in the limited cavitation flow regime, and that for flows of the same liquid around geometrically similar bodies dynamically similar growths of individual bubbles cannot be expected to obtain.

The effects of body size on cavitation were then investigated experimentally for two families of simple shapes in a steady rectilinear flow. The first experiments were performed on a family of 12% thick symmetrical Joukowski hydrofoils of constant chord which spanned the High Speed Water Tunnel test section. Next, R. W. Kermeen[3] supplied some experimental results for a series of right circular cylinders with hemispherical noses in axially symmetric flow.

The important results of the experiments may be summarized as follows: First, it was observed in connection with the high-speed motion picture studies that different cavitation numbers were required to obtain similar cavitation development on bodies of different size. This behavior was then confirmed at one free stream velocity for a range of cavitation numbers. Second, it was found that the cavitation number for the inception of cavitation increased with free stream velocity and, in certain instances, for constant velocity, the incipient cavitation number was found to increase with the size of the body.

PART II

THEORETICAL INVESTIGATIONS

Introduction to Theory

The experimental results summarized above show that the cavitation number for incipient cavitation exhibits systematic changes with variations in the free-stream velocity, and that for some conditions the incipient cavitation number at constant free-stream velocity changes with the scale of the body. It is the purpose of this section to investigate the conditions for incipient cavitation by analytical means so that more precise ideas can be obtained about the relationships between the parameters which influence the behavior of the cavitation.

The question of how a bubble grows from its original small nucleus to a macroscopic size is a dynamic problem, since the observed variations in the inception of cavitation are to be ascribed to differences in the transient tensions on the water produced by changes in body length and free stream velocity. The equation of motion for a spherical bubble of radius R(t) in an unlimited incompressible inviscid liquid is

$$R\ddot{R} + \frac{3}{2}\dot{R}^2 = \left[p(R) - P(t)\right]/\rho \quad , \tag{1}$$

where ρ is the liquid density, p(R) is the liquid pressure at the bubble wall, and P(t) is the external pressure field in the liquid far from the bubble. The superscribed dots, as usual, stand for differentiations with respect to time. Let σ be the surface tension of water, p_v the vapor pressure corresponding to the temperature of the liquid, and p_a the initial air pressure within the bubble before any growth from its initial size R_o has occurred. If the bubble is assumed to expand under isothermal conditions, then

$$p(R) = p_v - \frac{2\sigma}{R} + p_a\left(\frac{R_o}{R}\right)^3 \quad . \tag{2}$$

P(t) will be determined by the flow over the solid body.

Basic Assumptions and Definitions

Before proceeding with the detailed formulation of the theory, a statement of the basic assumptions underlying the whole analysis is required.

First, viscous effects are entirely neglected in the present work. For example, it is known that the minimum pressures in the liquid occur on the immersed body. In fact, the pressures decrease slightly as one proceeds through the boundary layer toward the body.[4] In view of the very small nucleus size it would seem that at least in the initial stages of bubble growth the phenomena might be restricted entirely to the boundary layer. The consideration of boundary layer effects requires further experimental information which is now being accumulated. The present discussion will not take them into account.

Second, the interaction between the flow around the growing bubble and the flow of the liquid around the immersed body is not considered.[5] Thus, the motion of the expanding bubble will be treated as though the liquid is infinite in all directions and the velocity and pressure relationships on the model will ignore the presence of cavitation. The effect of the flow around the body is related to the bubble growth through the $P(t)$ term in the equation of motion for the bubble.

Third, the bubble is assumed to move with the fluid. For the very small bubbles considered here, buoyant forces are small and the viscous drag will be high so that any relative motion between the bubble and the water will be very small.

Fourth, the bubbles are assumed to be spherical.

In this study it is supposed that cavitation is initiated from small nuclei* which contain air or water vapor, or both, stabilized on small, solid particles in the liquid. In the noncavitating flow regime it is assumed that the nuclei do not have an opportunity to grow into bubbles of macroscopic or visible size. The difference, then, between the noncavitating and cavitating flow regimes is that in the latter, the nuclei are exposed to a pressure environment favorable to bubble growth for a period sufficient to allow for the appearance of macroscopic bubbles. The appearance of macroscopic bubbles depends upon the response of the nuclei to the transient low pressure created by the flow of water around the body. This bubble growth problem will be determined by two conditions. First, the initial conditions $\dot{R}(0) = 0$ and $R(0) = R_o$ will be prescribed.

---

*It seems probable that the nuclei in a liquid have a range of sizes, but it will be assumed here that all nuclei are of equal effective radius R_o. Their size will be estimated in a subsequent section.

Second, the pressure-time relationship or "forcing function" which acts on the nuclei and promotes their growth is prescribed if one knows the pressure distribution around the immersed body, the body size, the free stream velocity, and the free stream static pressure. This simple determination of the forcing function is a consequence of the fundamental assumptions listed above.

For a given flow situation, the time available for bubble growth is fixed by the size of the solid body and the free stream velocity. Incipient cavitation will be said to exist if a nucleus grows from its initial radius R_o to a radius of one millimeter during the time it is exposed to the low pressure which favors growth. This value for the final bubble radius was selected because a bubble of one millimeter is visible to the unaided eye and this arbitrary bubble size is of the same order of magnitude as the bubbles of visible incipient cavitation on bodies in the water tunnel. Using this experimentally derived estimate, one can now ask: Given a fixed time for growth, determined by the free stream velocity and body size, what will be the free stream static pressure p_o (and hence K) at which the final bubble radius will be one millimeter?

Stability of Gas Nuclei

For practically all cases of technical interest, the water will contain dissolved air. Accordingly, the nuclei will contain air as well as water vapor. However, if surface tension forces act on these small bubbles, the air will be driven from the nuclei into solution with the surrounding water.[6] On the other hand, a stable nucleus can exist if air or vapor bubbles are attached to small solid particles in the liquid. In this case the effective surface tension must be zero. Therefore, if the effective surface tension is initially zero, the nuclei can exist indefinitely, and by Henry's Law[7] the initial air pressure in the gas pocket is proportional to the concentration of air dissolved in the water. As the bubble grows from its initial effective radius R_o, the surface tension will increase to the full value $2\sigma/R$. The required behavior of the surface tension may be approximated by $p_\sigma = 2S(R,\sigma)/R$ where the "surface tension law", $S(R,\sigma)$, is characterized by $S(R_o,\sigma) = 0$ and $S(R_1,\sigma) = \sigma$. Let R_1 be that bubble radius at which the surface tension law first achieves its full value and put $R_1 = nR_o$. The simplest assumption which will approximate the

complex variation of the surface tension law with bubble growth is that $S(R,\sigma)$ is a linear function of R. Then $S = (R - R_o)\sigma/R_o(n-1)$ for $R_o \leq R \leq nR_o$ and $S = \sigma$ when $R \geq nR_o$. If one puts $r = R/R_o$, then the surface tension law can be written in the form

$$S = \begin{cases} \dfrac{r-1}{n-1}\sigma \ , & 1 \leq r \leq n \ , \\ \sigma \ , & r \geq n \ . \end{cases} \tag{3}$$

It must be borne in mind that the surface tension law defined above is in a sense an attempt to account for an average behavior of a large number of nuclei of many possible initial sizes. Compared with the atomic or molecular scale, the nuclei are macroscopic structures and hence the laws of surface tension for macroscopic systems are applicable. It has been argued that in order that such systems may exist in a stable state it is necessary to add a solid phase to the gas-water system, and this has resulted in the introduction of another parameter, namely, the slope, 1/n, of the surface tension law. To ascribe an average behavior to such a large number of nuclei with many possible initial sizes is reasonable because experiments show that the zone of cavitation numbers at which cavitation starts is very narrow. Thus it is possible to assign a definite value of the cavitation number for the inception of cavitation for a given flow situation.

Primary Parameters and Pressure-Time Relationships

The problem then is to study the behavior of the "average" nucleus in the transient pressure regions caused by the flow of the nuclei-containing water around submerged bodies of various sizes at various flow velocities. Thus, the relationships between several parameters must be studied in order to obtain approximate quantitative results which may then be used to guide further experimental work. In particular, one must study the effects upon incipient cavitation of bubble air content, p_a, of the nucleus size, R_o, and of changes in the slope of the surface tension law (1/n). Furthermore, estimates for the initial radius will be found to depend upon the nucleus air content and the slope of the surface tension law, so that all of these factors are interrelated. However, it will be possible to make some theoretical conclusions about the effects of air content and surface tension law slope. To test such findings more detailed experimental

results are required. Unfortunately, there are at present almost no reliable experimental data for the effect of dissolved air content upon the inception of cavitation. Studies are now under way for determination of the effect of dissolved air content on incipient cavitation.

With regard to pressure-time relationships, no exact account will be taken of the many pressure distributions which can arise from all of the various body shapes that one may wish to consider in a liquid flow. However, the general pressure change, first falling and then rising, common to all such bodies, will be approximated by two parabola-like curves joined at the point of minimum pressure. The term "parabola-like" is used because the actual functions used will be parabolic in time and the resulting spatial pressure distributions will differ slightly from the true parabolic shape. Two curves joined at the minimum pressure point are used so that actual pressure distributions, which are seldom symmetrical about the minimum pressure point, can be more closely matched. It is the general qualitative behavior of the many possible pressure distributions that is of importance here. No attempt will be made to find an exact forcing function for any specific body shape.

Next, certain conditions will be determined which will enable the "parabolic" pressure distribution to be replaced by a dynamically equivalent step function pressure distribution. The detailed numerical integrations of the equation of motion for the bubble will be made by using this further simplification. Two distinct advantages are gained by the use of the step function. First, it turns out that for a given n, or surface tension law slope, if the parabolic approximation is used, a three parameter family of solutions for Eq. (1) must be found. However, when the step function pressure distribution is used, only a two parameter family of solutions is required. Second, the use of the equivalent step function allows one to find certain important relationships between the primary parameters involved in the problem. These relationships are not readily determined if the pressure is not constant during some time interval.

It was mentioned above that the only connection between the bubble growth and the liquid flow over the body is the choice of P(t) in the equation of motion for the bubble wall. For the step function pressure distribution it is evident that P(t) can be written as

$$P(t) = \begin{cases} p_o & , \quad t < 0 \ , \\ p_o - \frac{1}{2}\rho V_o^2 a & , \quad t \geq 0 \ , \end{cases} \tag{4}$$

where p_o and V_o are the free stream static pressure and velocity, respectively, ρ is the liquid density, and a is the pressure coefficient in the low pressure region. Fig. 1 shows the step function pressure law.

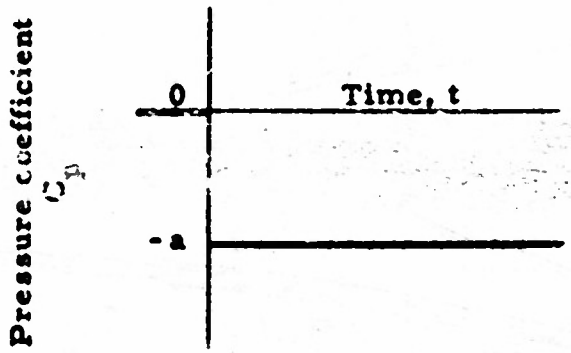

Fig. 1

If it is remembered that the bubble is assumed to grow isothermally, and if account is taken of Eqs. (3) and (4), the equation of motion (Eq. 1) becomes

$$R\ddot{R} + \frac{3}{2}\dot{R}^2 = \frac{1}{\rho}\left[p_v + p_a\left(\frac{R_o}{R}\right)^3 - 2\frac{S(R,\sigma)}{R} - p_o + \frac{1}{2}\rho V_o^2 a\right], \quad t > 0. \tag{5}$$

The initial conditions are $R(0) = R_o$ and $\dot{R}(0) = 0$.

Estimates for Initial Effective Bubble Radius

From inspection of Eqs. (3) and (5) one sees that the forces tending to retard the bubble growth are a maximum at $R = nR_o$. If the bubble grows in such a manner that R just reaches nR_o with zero velocity, it turns out that the time required for such growth will be infinite and cavitation will not occur. On the other hand, if the forces reach equilibrium when $R = nR_o$ the motion will have considerable momentum, and the bubble growth will be little influenced by the retarding forces. Cavitation will then be well started. One can use this condition of force equilibrium together with experimental values for cavitating flow to obtain an estimate of the initial radius R_o. Thus, setting the right hand side of Eq. (5) equal to zero, one finds that for $R = nR_o$

$$(a - K)\frac{1}{2}\rho V_o^2 + \frac{p_a}{n^3} - \frac{2\sigma}{nR_o} = 0 \ ,$$

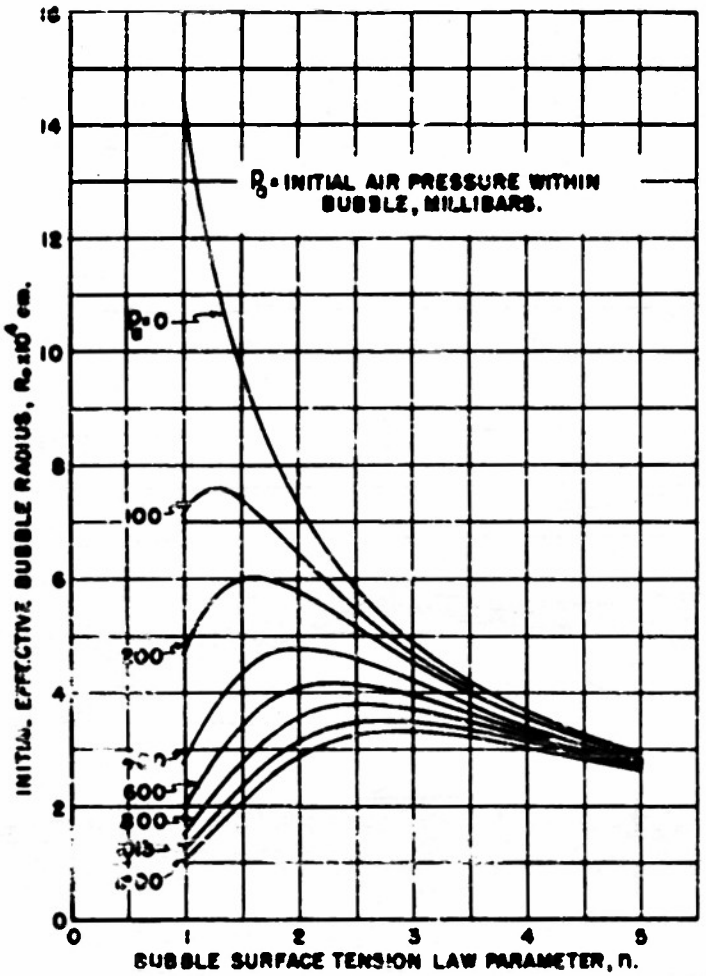

Fig. 2 - Estimates for the initial effective bubble radius under various dissolved air and surface tension law conditions

where K is the cavitation number, $(p_o - p_v)/(1/2\,\rho V_o^2)$. Experimental values of K and V_o were taken from the data for incipient cavitation number for the Joukowski hydrofoils,[1] and curves of R_o versus n for various air contents, p_a, were calculated. The results are shown in Fig. 2. (V_o = 30 fps = 914 cm/sec, K = 0.30, σ = 70 dynes/cm, a = 0.53). Inspection of the R_o vs. n curves shows that except for the case of no dissolved air in the water, the variations in the initial radius with the surface tension law slope are not large. Further, since R_o is given by

$$R_o = \frac{2\sigma}{n(a-K)(1/2\,\rho V_o^2) + p_a/n^2} \quad ,$$

an underestimate of the pressure difference (a - K) results in an overestimate of R_o. In using experimental values of (a - K) for incipient cavitation, one must recognize that such an underestimate of (a - K) is being made. The chief value of the calculations is that they show that an initial radius of the order of 10^{-4} cm is reasonable (Fig. 2).

Critical Conditions for Cavitation

As was mentioned above, the forces tending to retard bubble growth reach a maximum at $R = n R_o$. However, if the bubble motion acquires enough momentum before reaching this point, the bubble will grow through this critical region even if the net force acting on the bubble in this region tends to collapse it. On the other hand, for certain values of the coefficients in the equation of motion (5), the small radius $n R_o$ will not be greatly exceeded, and by definition the condition for incipient cavitation will not be fulfilled. In this section relationships will be derived between these coefficients which will define the threshold of visible cavitation.

Before deriving the relationships between the coefficients, the equation of motion will be rewritten in dimensionless form. If one puts $r = R(t)/R_o$ and $\tau = t\sqrt{2\sigma/\rho R_o^3}$ Eq. (5) becomes

$$r\frac{d^2r}{d\tau^2} + \frac{3}{2}\left(\frac{dr}{d\tau}\right)^2 = a + \frac{\gamma}{r^3} - \begin{cases} \dfrac{r-1}{(n-1)r}, & r \leq n, \\ \dfrac{1}{r}, & r \geq n, \end{cases} \tag{6}$$

where the "bubble driving parameter" a is given by

$$a = \frac{p_v - p_o + \frac{1}{2}\rho V_o^2 a}{2\sigma/R_o} = (a - K)\frac{R_o \rho V_o^2}{4\sigma}, \tag{7}$$

and the "air content parameter" γ is

$$\gamma = \frac{p_a}{2\sigma/R_o}. \tag{8}$$

The initial conditions are then

$$r(0) = 1 , \quad \frac{dr(0)}{d\tau} = 0 . \tag{9}$$

By recognizing that

$$r\frac{d^2r}{d\tau^2} + \frac{3}{2}\left(\frac{dr}{d\tau}\right)^2 = \frac{1}{2r^2}\frac{d}{dr}\left[r^3\left(\frac{dr}{d\tau}\right)^2\right]$$

one can write the first integral of Eq. (6) as

$$\frac{1}{2}r^3\left(\frac{dr}{d\tau}\right)^2 = \frac{\alpha}{3}(r^3-1) + \gamma \ln r - \begin{cases} \frac{1}{n-1}\left(\frac{r^3-1}{3} - \frac{r^2-1}{2}\right) & r \leq n \\ \frac{r^2}{2} - \frac{n^2+n+1}{6} , & r \geq n , \end{cases} \tag{10}$$

where the initial conditions, Eq. (9), have been used and the two integrals have been matched at $r = n$. Equation (10) simply states that the change in the kinetic energy during the expansion is equal to the work done in the course of the motion. If one lets $W(r)$ represent the terms on the right-hand side of Eq. 10, then for small enough values of the bubble driving parameter, α, the function $W(r)$ is very near a cubic polynomial, as shown schematically in Fig. 3. The value of r, for which W has its isolated minimum, will be called r_1. It can be shown that for n greater than 1 the minimum of W occurs at a value of r_1 greater than n. Since the kinetic energy is zero for $r = 1$, it will again be zero at the minimum of W if $W_{min} = 0$. It can also be shown that the time required for the bubble to grow to the value r_1, which corresponds to a zero minimum of W, is logarithmically infinite. Thus, if the bubble driving parameter, α, and the bubble air content parameter, γ, are chosen in such a way that $W_{min} = 0$, then cavitation will not occur under any circumstance. One may

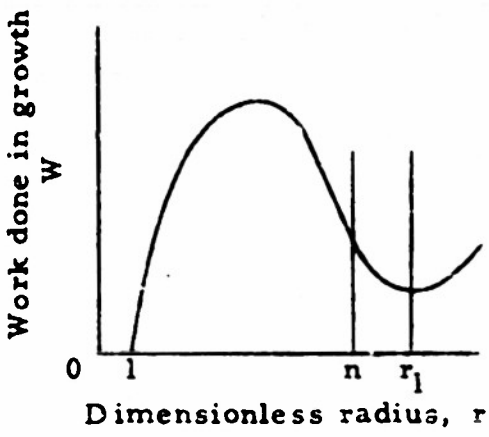

Fig. 3

call such values of the bubble driving parameter, a, and the bubble air content parameter, γ, critical values. These critical values are denoted by a_c and γ_c, respectively. A relationship between the critical values a_c and γ_c will now be found from the conditions $W(r_1) = 0$ and $dW(r_1)/dr = 0$.

From Eq.(10) the minimum conditions give

$$W(r_1) = \frac{a_c}{3}(r_1^3 - 1) + \gamma_c \ln r_1 - \frac{r_1^2}{2} + \frac{n^2+n+1}{6} = 0$$

and

$$\frac{dW(r_1)}{dr} = a_c r_1^2 + \frac{\gamma_c}{r_1} - r_1 = 0 .$$

Because the minimum occurs for $r_1 > n$, only the part of the integral (10) for $r \geq n$ is required. If r_1 is regarded as a fixed parameter, a_c and γ_c are given in the parametric form,

$$a_c = \frac{\frac{r_1^2}{2} - r_1^2 \ln r_1 - \frac{n^2+n+1}{6}}{\frac{r_1^3 - 1}{3} - r_1^3 \ln r_1} , \qquad (11)$$

and $$\gamma_c = r_1^2 - a_c r_1^3 .$$

The minimum value of r_1 corresponds to $\gamma_c = 0$ and the root of $0 = r_1^2 - a_c r_1^2$ of physical significance is $r_1 = 1/a_c$. Substitution of this result for r_1 into a_c (Eq. 11) gives

$$a_c^3 - \frac{n^2+n+1}{2} a_c^2 + 1/2 = 0 , \quad \gamma_c = 0 . \qquad (12)$$

Equation (12) has one real root for a_c. When a_c is real, it is expedient to solve for n in terms of a_c. Since $n \geq 1$, Eq. (12) gives for the positive root

$$n = \frac{1}{2}\left[\frac{\sqrt{8a_c^3 - 3a_c^2 + 4}}{a_c} - 1\right] .$$

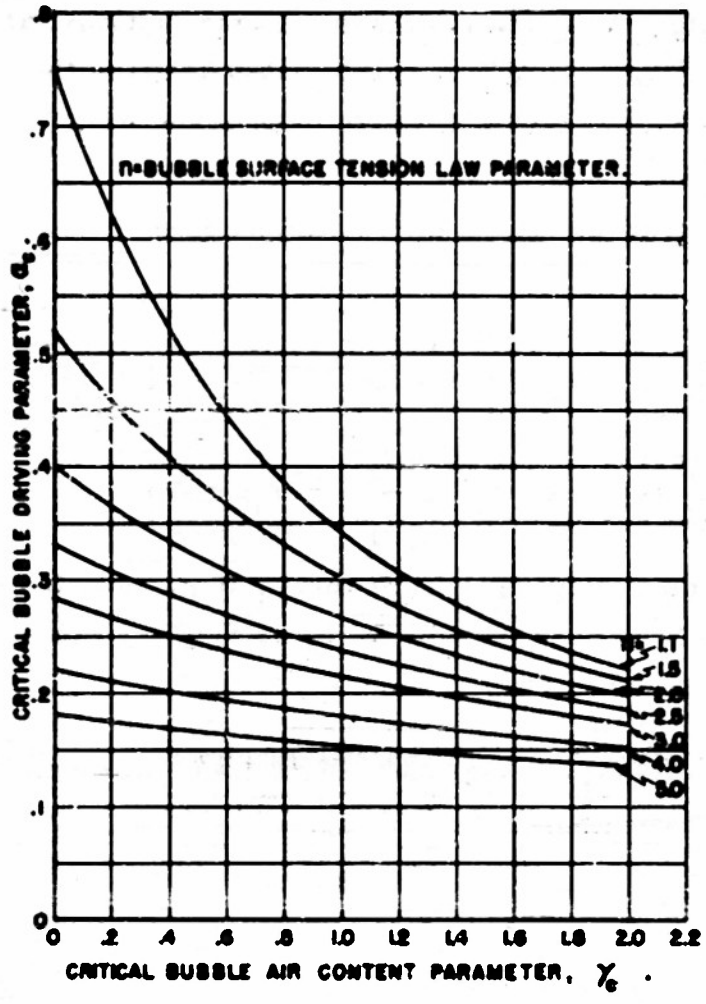

Fig. 4 - The critical conditions for the occurrence of cavitation

Taking values of α_c from 0.1 to 1.0, one finds the corresponding values of n and r_1. These results were plotted. For various fixed values of the surface tension slope number, n, the values of r_1 and α_c for $\gamma_c = 0$ were taken from this curve and then larger values of r_1 were selected to compute α_c and γ_c from Eqs. (11). The results of these computations are graphically presented in Fig. 4. These curves of the critical driving parameter, α_c, as a function of the critical air-content parameter, γ_c, are the loci of points for which the time required for a bubble to grow from its initial size to a size near nR_o^* (or larger) is infinite. For example, if for a given slope (1/n) of the surface tension law, a value of

---

*Actually, the growth is from $r = 1$ to $r = r_1 \geq n$ with $r_1 \ll 10n$.

α greater than α_c is chosen at a fixed value of the air content parameter, γ, a finite time will be required for a bubble to reach a definite radius. Further, if the slope of the surface tension curve is increased (n decreased) the bubble growth time increases without limit as α approaches α_c.

Numerical Calculations with the Step Function Pressure Law

In order that definite numerical calculations can be made, values of n and R_o must be chosen. If the original bubble is stabilized on only a portion of an unwetted solid particle, it seems plausible that the bubble must grow to several times its initial size before the surface tension law reaches its full value σ. For the present calculations a value of 5 will be taken for the parameter, n, in the surface tension law. If one takes account of the overestimate contained in the curves of R_o versus n (Fig. 2), a value for the initial effective radius, R_o, of 2×10^{-4} cm. seems reasonable.

In accordance with the definition of incipient cavitation given above, the bubble must grow to a macroscopic size of R = 1 millimeter. The total range of r, $(= R(t)/R_o)$ will then be from 1 to 500. The problem of determining the condition for incipient cavitation is now reduced to the following question. What time interval, as a function of the bubble-driving parameter α and the bubble air-content parameter γ is required for the bubble to reach a radius which is 500 times its initial value? To answer this question one must find a two-parameter family of solutions of Eq. (10) of the form $\tau = F(\alpha, \gamma)$. The dimensionless time parameter, τ, is a function of the body length, free stream velocity, and cavitation number. The air content parameter, γ, will be given and α, the bubble-driving parameter, is a function of the cavitation number and free stream velocity. Then if $\tau = F(\alpha, \gamma)$ is known, a trial and error procedure will give the incipient cavitation number when the free stream velocity is known.

Equation (10) is easily reduced to quadratures, so that the dimensionless time τ is given by

$$\tau = \int_1^5 \frac{r^{3/2}\,dr}{\sqrt{\frac{2}{3}\alpha(r^3-1) + 2\gamma \ln r - \frac{2}{n-1}\left(\frac{r^3-1}{3} - \frac{r^2-1}{2}\right)}} \qquad (13)$$

$$+ \int_5^{500} \frac{r^{3/2}\,dr}{\sqrt{\frac{2}{3}\alpha(r^3-1) + 2\gamma \ln r - 2\left(\frac{r^2}{2} - \frac{n^2+n+1}{6}\right)}}$$

The two integrals arise because of the change in the surface tension law at $r = n = 5$. Since the variations in τ are required for small changes in α and γ, approximate representations for Eq. (13) will be limited in value for those cases where α is near the critical bubble-driving parameter α_c. In any event, numerical integrations have to be precise for the first integral in Eq. (13).

For the range of the air content parameter, γ, from 0 to 1.8, with corresponding values of the bubble-driving parameter, α, from 0.145 to 0.230, ninety-eight integrations of Eq. (13) were carried out on an I. B. M. calculator. From these results the functional relationship, $\tau = F(\alpha, \gamma)$, represented by Eq. (13) was plotted as in Fig. 5. Tabulated data, from which the figure was made, are given in Table I.

After the above trial and error calculations for incipient cavitation number versus velocity have been made for different values of the air content parameter γ, comparisons between experimental results and the calculations for the given shape could be used to obtain a measure of the success with which the surface tension law parameter, n, was chosen. It will be noticed from Fig. 4, that the slopes of the curves for critical bubble-driving parameter, α_c, versus the critical bubble air content parameter, γ_c, are steepest for low values of the surface tension law parameter. Thus, the cavitation number for incipient cavitation will be smaller for steeper slopes of the surface tension law, $S(R, \sigma)$, than it will for a surface tension law with more gradual slope (large n). If sufficiently reliable data are available, a comparison with the calculated curves for incipient cavitation will suggest a better choice for the effective surface tension law parameter, n. Because there are almost no reliable data at this time, these alterations of the calculations will not be made here.

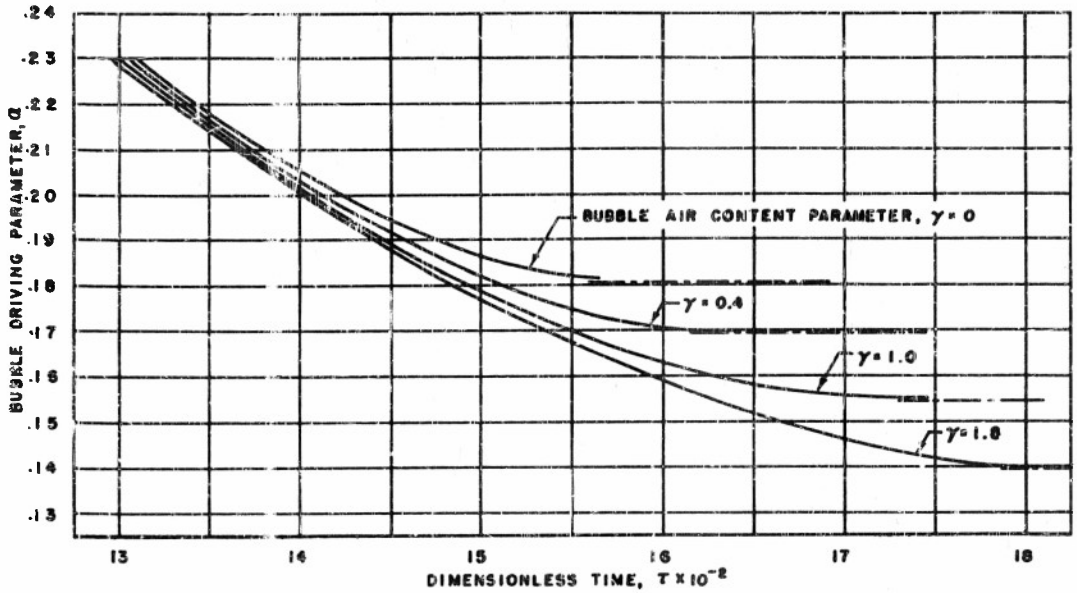

Fig. 5 - Graph of the function $\tau = F(\alpha, \gamma)$

TABLE I - TIME REQUIRED FOR A BUBBLE GROWTH, R/R_0, OF 492.75 FROM THE I.B.M. DIGITAL COMPUTER

γ, Bubble Air Content Parameter.	α, Bubble Driving Parameter. .145	.150	.155	.160	.165	.170	.175	.180	.185	.190	.200	.210	.220	.230	α_0 for $\tau \to \infty$ for the given values of γ
0										1474.6	1424.6	1382.6	1345.3	1311.4	.1207
.2									1491.9	1445.1	1418.8	1378.2	1341.7	1308.3	.1754
.4							1544.1	1511.8	1484.2	1459.4	1414.8	1375.1	1339.1	1306.2	.1696
.6						1567.1	1533.6	1505.0	1479.2	1455.3	1411.8	1372.7	1337.1	1304.4	.1641
.8					1592.4	1557.2	1527.3	1500.3	1475.4	1452.1	1409.4	1370.7	1335.5	1303.0	.1593
1.0					1582.6	1551.1	1522.8	1496.7	1472.4	1449.5	1407.3	1369.1	1334.0	1301.7	.1550
1.2				1609.9	1576.4	1546.6	1519.3	1493.8	1469.9	1447.4	1405.6	1367.6	1332.8	1300.6	.1509
1.4			1639.3	1603.5	1572.0	1543.2	1516.5	1491.4	1467.8	1445.5	1404.1	1366.3	1331.7	1299.6	.1470
1.6		1671.2	1632.6	1599.0	1568.5	1540.4	1514.1	1489.4	1466.0	1443.9	1402.7	1365.2	1330.6	1298.7	.1430
1.8	1706.1	1663.7	1627.7	1595.3	1565.6	1538.0	1512.0	1487.6	1464.4	1442.4	1401.5	1364.1	1329.7	1297.9	.1394

DIMENSIONLESS TIME, $\tau \cdot$

Properties of the "Parabolic" Pressure Function

As noted previously, the step function results will be related to the growth of a bubble under a more realistic pressure-time forcing function. The important general features of many such actual forcing functions can be qualitatively represented by two functions which are parabolic in time. One function which decreases from $C_p = 0$ to $C_p = -b$ and another function which increases from $C_p = -b$ to $C_p = 0$ will be employed. Two functions are used because the pressure distributions around actual bodies are seldom symmetrical in the streamwise direction. Fig. 6 shows the parabolic pressure distribution. The required results for the "parabolic" pressure distribution will now be obtained.

Decreasing part, $0 \geq C_p \geq -b$:

The equation of a time parabola which decreases from $C_p = 0$ to $C_p = -b$ in a time interval T, may be written as

$$C_p(t) = -b\left[2\frac{t}{T} - \left(\frac{t}{T}\right)^2\right], \tag{14}$$

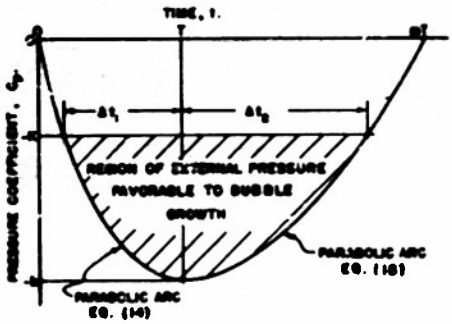

where t is any time in the interval $0 \leq t \leq T$ (Fig. 6). From the Bernoulli equation $dx/dt = V = V_o\sqrt{1 - C_p(x)}$, where x is the distance along the stream line adjacent to the body. Under the conditions $x = x(t)$, with $dx/dt \neq 0$ one may write $dx/dt = V_o\sqrt{1 - C_p(t)}$. If $x(0) = 0$ and $x(T) = \ell_1$, one obtains

Fig. 6 - The time-parabolic pressure law

$$\frac{\ell_1}{T V_o\sqrt{b}} = \int_0^1 \sqrt{\frac{1+b}{b} - \left(1 - \frac{t}{T}\right)^2}\; d\left(\frac{t}{T}\right)$$

or

$$T = \frac{2\ell_1}{V_o\left(\sqrt{\frac{1}{b}} + \frac{1+b}{5}\sin^{-1}\sqrt{\frac{b}{1+b}}\right)\sqrt{b}} \tag{15}$$

When $C_p = -K$, that is, the pressure coefficient on the body is equal to minus the cavitation number for the flow, the pressure in the water around the bubble is equal to the vapor pressure of the water. Inspection of Eq. (5) shows that the bubble can not start to expand until it has reached a point on the model where $C_p = -K$. The region for which $C_p \leq -K$ will be called the region of "favorable environment" for bubble growth. Thus the time that is of concern here is the time during which the bubble is in a favorable environment. The value of (t/T) for which $C_p = -K$ is obtained directly from Eq. (14). If t_1 is the required value of the time, then

$$1 - \frac{t_1}{T} = \sqrt{\frac{b-K}{b}} \quad ,$$

but the time interval Δt_1 spent by the bubble in the favorable environment is $(T - t_1)$. Hence $\Delta t_1 = T\sqrt{(b-K)/b}$, or substituting for T one finds

$$t_1 = \frac{2\ell_1\sqrt{b-K}}{V_o\left(\sqrt{b} + (1+b)\sin^{-1}\sqrt{\frac{b}{1+b}}\right)} \quad . \tag{16}$$

The relationship $x = x(t)$ can be found by suitably altering the limits of integration in the integral leading to Eq. (15). If Eq. (15) is solved for ℓ_1 and divided into the result for $x = x(t)$, one obtains

$$\frac{x}{\ell_1} = 1 - \frac{(1-\frac{t}{T})\sqrt{\frac{1+b}{b} - (1-\frac{t}{T})^2} + \frac{1+b}{b}\sin^{-1}(1-\frac{t}{T})\sqrt{\frac{b}{1+b}}}{\sqrt{\frac{1}{b}} + \frac{1+b}{b}\sin^{-1}\sqrt{\frac{b}{1+b}}} \quad . \tag{17}$$

Increasing part, $-b \leq C_p \leq 0$:

For the portion of the pressure distribution downstream from the minimum pressure point, one can write

$$C_p(t) = \frac{b}{(m-1)^2}\left[\left(\frac{t}{T} - 1\right)^2 - (m-1)^2\right] \quad , \tag{18}$$

where $1 \leq \frac{t}{T} \leq m$. Thus, $C_p(T) = -b$ and $C_p(mT) = 0$. In a manner similar to that used in obtaining Eq. (15), the analogous result

$$(m-1)\,T = \frac{2\,\ell_2}{V_o\left(\sqrt{\frac{1}{b}} + \frac{1+b}{b}\,\sin^{-1}\sqrt{\frac{b}{1+b}}\right)\sqrt{b}} \quad , \tag{19}$$

is obtained. Here ℓ_2 is the distance along the stream line next to the body from the point where $C_p = -b$ to the point where again $C_p = 0$. and T is given by Eq. (15). The time t_2 at which $C_p = -K$ is obtained from Eq. (18)

$$\frac{t_2}{T} - 1 = (m-1)\sqrt{\frac{b-K}{b}} \quad .$$

The period spent by the bubble in the favorable environment for this portion of the pressure distribution is given by $\Delta t_2 = (t_2 - T)$. Substitution for $(m-1)T$ from Eq. (19) yeilds

$$\Delta t_2 = \frac{2\,\ell_2\sqrt{(b-K)}}{V_o\left[b + (1+b)\,\sin^{-1}\sqrt{\frac{b}{1+b}}\right]} \quad . \tag{20}$$

As before, the space-time relationship can be found in a manner similar to that employed in deriving Eq. (17). Thus,

$$\frac{x}{\ell_2} = \frac{\left(\frac{t}{T}-1\right)\sqrt{\frac{1+b}{b} - \left(\frac{\frac{t}{T}-1}{m-1}\right)^2} + \frac{1+b}{b}\sin^{-1}\left(\frac{\frac{t}{T}-1}{m-1}\right)\sqrt{\frac{b}{1+b}}}{\sqrt{\frac{1}{b}} + \frac{1+b}{b}\,\sin^{-1}\sqrt{\frac{b}{1+b}}} \quad , \tag{21}$$

where x is measured along the stream line from the point for which $C_p = -b$. From Eq. (15) the expression for T can be put into Eq. (19) to find m. This substitution gives

$$(m-1) = \frac{\ell_2}{\ell_1} \quad . \tag{22}$$

The "parabolic" curves are compared with the Joukowski and the "Hemisphere" experimental pressure distributions in Figs. 8 and 10. Equations (16) and (20) can be added to find the total time, $\Delta t = \Delta t_1 + \Delta t_2$, that a bubble spends in the whole region of favorable environment, and one finds

$$\Delta t = \frac{2(\ell_1 + \ell_2)\sqrt{b - K}}{V_o\left(\sqrt{b} + (1+b)\sin^{-1}\sqrt{\frac{b}{1+b}}\right)} \tag{23}$$

It is this value of the time Δt which determines the dimensionless time τ. For a given pressure distribution, ℓ_1, ℓ_2, and b are known quantities and V_o, the free stream velocity, will be given so that K is the only unknown factor required to find Δt or τ.

Dynamic Equivalence between the Step and "Parabolic" Pressure Laws

The preceding preliminary calculations now make it possible to approximate the relationship which must obtain between the idealized step function pressure distribution and the more realistic "parabola-like" pressure distribution if the essential features of the bubble growths are to be the same in both cases. The matching will consist of two parts. First, the time spent by the bubble in the low pressure region will be taken to be the same for both the step function and the parabolic pressure laws. Second, the equation of motion (1) will be integrated in closed form by approximate means for both the step function and the parabolic pressure laws. The two approximate bubble histories will be said to be dynamically equivalent when the total bubble growths under the two pressure laws are equal. These two conditions will result in approximations of the required relationships between the step and parabolic pressure functions.

The first point of comparison for the two pressure laws is the relationship between the time intervals during which the nucleus is exposed to the favorable environment in each case. It will be specified that the time spent by the bubble in the favorable invironment shall be the same for both the step function pressure law and the "parabolic" pressure distribution. In both instances the free stream velocity, V_o, will be identical. From Eq. (4), the pressure coefficient for the pressure step is

$$C_p = \begin{cases} 0 & \text{for } t < 0, \text{ or } x < 0, \\ -a & \text{for } t \leq 0, \text{ or } x \leq 0, \end{cases} \qquad (24)$$

If the bubble is assumed to grow in an interval $0 \leq x \leq \lambda$ then the same reasoning which gave Eq. (15) gives $t = \dfrac{\lambda}{V_o\sqrt{1+a}}$, where Δt is the total time during which the bubble is exposed to the low pressure and λ is the distance along a stream line traversed by the bubble in the time Δt. Equating this result to the Δt of Eq. (23) gives

$$\frac{\lambda}{\sqrt{1+a}} = \frac{2(\ell_1 + \ell_2)\sqrt{b-K}}{\sqrt{b} + (1+b)\sin^{-1}\sqrt{\frac{b}{1+b}}} \qquad (25)$$

If a relationship between a and b can be found, then λ will be given in terms of known quantities.

The second point of comparison is the requirement that the total bubble growth in the time interval of favorable environment must be the same for the two pressure functions. This requirement, which will result in a relationship between a and b, will be called dynamical equivalence. The a priori derivation of an exact condition for the dynamical equivalence of the two cases is formidable in view of the fact that to obtain such a precise result the equation of motion (1) must be integrated in exact analytical form. It will be worthwhile to use an approximate method of integration due to M. S. Plesset.[8] Plesset's method, while lacking rigorous justification, has been shown to give results in close agreement with precise numerical results if the right-hand side of the dynamical Eq. (1) is a function which increases exponentially with time. In this instance, Plesset's method approximated the exact numerical results within 0.3% for sufficiently large values of the bubble growth time. On the other hand, if the pressure is constant, it can be shown that this approximation will give the final bubble radius with an error of about 5%.* Thus, if the right-hand side of the equation of motion, Eq. (1), is a monotonic function of

*This comparison approximates the effect of surface tension for bubbles growing through the specified size range because, when surface tension and air content are negligible, Plesset's method is exact. This comparison was made for bubbles with surface tension and initial internal air pressure.

time, it is evident that a suitable approximation for the final bubble size will result. Plesset's method is based on the supposition that the right-hand side of the equation of motion is a monotonic function of time. It is unfortunate that this condition will not be entirely satisfied here. After obtaining the required approximate result, it will be used to define a pair of dynamically equivalent pressure distributions so that numerical integrations can be performed to test the reasonableness of the approximate method.

The equations of motion applied to each case differ only in the form of the forcing function on the right-hand side, because in one case a step function is taken while in the other case a "parabolic" dependence is assumed. Thus, it seems reasonable that in comparing the behavior in the two cases, one can discard the surface tension and air content terms. This approximation may be partially justified by recognition of the fact that both the surface tension and the air content terms decrease very rapidly as the bubble grows. Thus Eq. (1) can be written in the form

$$R\ddot{R} + \frac{3}{2}\dot{R}^2 = g(t) \quad , \tag{26}$$

where g(t) is given for the step function case by

$$g(t) = \begin{cases} \frac{1}{2} V_o^2 (-K) \quad , & t < 0 \ , \\ \frac{1}{2} V_o^2 (a - K) \ , & t \geq 0 \ ; \end{cases} \tag{27}$$

and for the parabolic case by

$$g(t) = \frac{1}{2} V_o^2 b \left[\frac{b-K}{b} - \left(1 - \frac{t}{T}\right)^2 \right] \ , \tag{28}$$

with

$$0 \leq \left(1 - \frac{t}{T}\right) \leq \sqrt{\frac{b-K}{b}} \quad .$$

Equation (28) accounts for only the portion of the parabolic pressure curve lying upstream from the minimum pressure point which is in the region of favorable environment. The growth in the second portion of the parabolic pressure curve will be accounted for by approximating the slope of the growth curve at the minimum pressure point and multiplying this

slope by the time interval of favorable environment Δt_2 (Eq. 20).

Plesset's approximate integration method is based upon the condition that in Eq. (26) g(t) is a function that does not permit the acceleration of the bubble wall $\ddot{R}$ to become negative; then

$$R\ddot{R} = g(t) - \frac{3}{2}\dot{R}^2 \geq 0. \tag{29}$$

Consequently:

$$\dot{R}^2 \leq \frac{2}{3} g(t) \quad , \quad \text{or}$$

$$\dot{R} \leq \sqrt{\frac{2}{3} g(t)} \quad . \tag{30}$$

Integration of (30) gives

$$R - R_o \leq \int_{t_0}^{t} \sqrt{\frac{2}{3} g(\xi)}\, d\xi \quad , \tag{31}$$

where R_o is the radius at the initial time t_o. Now define a function $\varphi(t)$ such that

$$R - R_o = \varphi(t) \int_{t_0}^{t} \sqrt{\frac{2}{3} g(\xi)}\, d\xi = \varphi(t)\, I(t) \quad . \tag{32}$$

Because of Eq. (31), the function $\varphi(t)$ is of bounded variation:

$$0 \leq \varphi(t) \leq 1 \quad . \tag{33}$$

Equation (32) is a formal solution to Eq. (26). Accordingly, substitution of (32) into Eq. (26) gives the exact differential equation,

$$(R_o + \varphi I)(\ddot{\varphi} I + 2\dot{\varphi} \dot{I} + \varphi \ddot{I}) + \frac{3}{2}(\dot{\varphi} I + \dot{I}\varphi)^2 = \frac{3}{2} \dot{I}^2 \quad . \tag{34}$$

Equation (34) will now be approximated with the assumptions that

$$\ddot{\varphi} I + 2\dot{\varphi} \dot{I} \ll \varphi \ddot{I} \quad ,$$

$$\dot{\varphi} I \ll \varphi \dot{I} \quad ,$$

and $$R_o \ll \varphi I \quad .$$

A first approximation for φ is then given algebraically by Eq. (34).

Solving for φ yields,

$$\varphi \approx \frac{1}{\sqrt{1 + \frac{2\,\dot{I}\,\ddot{I}}{3\dot{I}^2}}} \tag{35}$$

This result, together with Eq. (32), gives the required approximate integration. In order that the parabolic case can be treated by means of the linear extension outlined above, the derivative $dR(t)/dt$ must be found. If one takes account of the inequalities preceding Eq. (35) the derivative is given by $\dot{R} \approx \varphi \dot{I}$. From the results following Eq. (19) $\Delta t_2 = (t_2 - T) = (m - 1)\, T \sqrt{(b - K)/b}$ so that the linear growth to be added is

$$\dot{R}(T)\ \Delta t_2 \approx \varphi \dot{I}\,(m - 1)\, T \sqrt{\frac{b - K}{b}}$$

Hence the total growth in the parabolic case is

$$R - R_o \approx \varphi(T) \left[I(T) + \dot{I}(T)(m - 1)\, T \sqrt{\frac{b - K}{b}} \right] \tag{36}$$

Substituting the equation for $g(t)$ (Eq. 28) into the integral for $I(t)$, one finds,

$$I(t) = \int_{1 - \sqrt{\frac{b-K}{b}}}^{\frac{t}{T}} \sqrt{\frac{2}{3} - \frac{1}{2} V_o^2 b \left[\frac{b - K}{b} - (1 - u)^2 \right]}\, du \ ;$$

or putting $y = (1 - u) \sqrt{\frac{b}{b - K}}$,

$$I(t) = - T V_o \sqrt{\frac{(b-K)^2}{3b}} \int_1^{(1 - \frac{t}{T}) \sqrt{\frac{b}{b-K}}} \frac{}{\sqrt{1 - y^2}}\, dy = - \frac{T V_o}{2} \sqrt{\frac{(b-K)^2}{3b}} \left[- \frac{\pi}{2} \right.$$

$$\left. + \sin^{-1} (1 - \tfrac{t}{T}) \sqrt{\tfrac{b}{b-K}} + (1 - \tfrac{t}{T}) \sqrt{\tfrac{b}{b-K}} \sqrt{1 - \tfrac{b}{b-K} (1 - \tfrac{t}{T})^2} \right] .$$

Hence,

$$I(T) = \frac{\pi}{4} T V_o \sqrt{\frac{(b-K)^2}{3b}} \tag{37}$$

From

$$\dot{I}(t) = V_o \sqrt{\frac{b-K}{3}} \sqrt{1 - \frac{b}{b-K}\left(1-\frac{t}{T}\right)^2} \quad \text{and} \quad \ddot{I}(t) = -\frac{V_o\left(1-\frac{t}{T}\right)\sqrt{\frac{b-K}{3}}}{T\sqrt{1-\frac{b}{b-K}\left(1-\frac{t}{T}\right)^2}}$$

it follows that,

$$\dot{I}(T) = V_o \sqrt{\frac{b-K}{3}} \quad \text{and} \quad \ddot{I}(T) = 0 \ . \tag{38}$$

From Eq. (38) and Eq. (35), $\varphi(T) \approx 1$ so that $R - R_o$, Eq. (36), becomes

$$R - R_o \approx T V_o \left(\frac{\pi}{4} + m - 1\right)\sqrt{\frac{(b-K)^2}{3b}} \tag{39}$$

for the parabolic case.

$$I(t) = \int_0^t \sqrt{\frac{2}{3}\ \frac{1}{2} V_o^{\,2}(a-K)}\ dt' \tag{40}$$

Because the time spent in the favorable environment is the same in this case as it is in the parabolic case, the time interval for Eq. (40) is equal to the Δt of Eq. (23). It is easy to see that $\Delta t = mT\sqrt{(b-K)/b}$ so that

$$I(\Delta t) = m V_o T \sqrt{\frac{(a-K)(b-K)}{3b}} \ . \tag{41}$$

Inspection of Eq. (40) shows that $\ddot{I}(t) = 0$ so that $\varphi(t) = 1$. For this case Eq. (32) alone suffices to give the approximate integration required, and hence

$$R - R_o \approx m V_o T \sqrt{\frac{(a-K)(b-K)}{3b}} \tag{42}$$

The requirement for dynamical equivalence can be applied to Eqs. (39) and (42) to give

$$m\sqrt{a-K} \approx \left(\frac{\pi}{4} + m - 1\right)\sqrt{b-K} \quad . \tag{43}$$

Thus, the relative shapes of the step and the parabolic pressure distributions are now specified by

$$\frac{\lambda}{\sqrt{1+a}} = \frac{2(\ell_1 + \ell_2)\sqrt{b-K}}{\sqrt{b} + (1+b)\sin^{-1}\sqrt{\frac{b}{1+b}}} \quad , \tag{25}$$

$$\sqrt{a-K} \approx \left(\frac{\pi/4 + m - 1}{m}\right)\sqrt{b-K} \quad , \tag{43}$$

and

$$(m-1) = \ell_2/\ell_1 \quad . \tag{22}$$

The above matching conditions were checked for one case of incipient cavitation on the two inch Joukowski hydrofoil. From the trial and error calculations presented below (p. 29), it was found that when the free stream velocity is 16 meters per second the incipient cavitation number, K, is 0.403, and hence the bubble-driving parameter, a, is 0.190 and the dimensionless time, τ, is 1400. The equation of motion (1) was integrated for the case where the air content parameter, γ, is 1.0 and the P(t) term is composed of the parabolic laws (16) and (20). The numerical solution gives a bubble diameter of 2/3 mm. at the end of the specified time interval. If the matching had been exact the final bubble diameter would have been 2 mm. The two results are comparable, well within an order of magnitude. Hence, one may conclude that the matching condition (Eq. 43) between the step and parabolic pressure laws will give reasonable results for the present application.

Scaling Laws for Incipient Cavitation at High Free Stream Velocity ($V_o \rightarrow \infty$)

It is now possible to obtain a relationship for cavitation scale effect for very large values of the velocity, V_o. As the free stream velocity, V_o, becomes very large, the bubble-driving parameter, a, (see Eq. 7) increases as V_o^2. From Eq. (23) it is clear that the time, Δt (and hence τ since $\tau = \Delta t \sqrt{2\sigma/\rho R_o^3}$) decreases as $1/V_o$. Hence for $a \gg 1$,

Eq. (13) can be approximated by

$$\tau \approx \sqrt{\frac{3}{2a}} \int_1^{500} dr \quad , \tag{44}$$

where $a = (a - K) \dfrac{R_o \rho V_o^2}{4\sigma} = \left(\dfrac{\pi/4 + m - 1}{m}\right) \dfrac{R_o \rho V_o^2}{4\sigma} (b - K)$.

This result for a follows from Eqs. (7) and (43). From Eq. (23) the relation,

$$\tau = \frac{2(\ell_1 + \ell_2) \sqrt{b - K}}{V_o \left(\sqrt{b} + (1 + b) \sin^{-1} \sqrt{\dfrac{b}{1+b}}\right)} \sqrt{\frac{2\sigma}{\rho R_o^3}} \quad ,$$

will be used for τ in Eq. (44). For geometrically similar bodies, $(\ell_1 + \ell_2)$ will be some constant multiplied by the characteristic body length L. Using this fact and substituting for τ and a into Eq. (44), one finds

$$\frac{L \sqrt{b - K}}{V_o} \approx \frac{C}{\sqrt{(b - K) V_o^2}} \quad . \tag{45}$$

where C is a constant. Suppose now that a given body running at very high velocity has a characteristic length L_o and is found to have an incipient cavitation number K_o. Then if another similar body in high speed flow has length L and incipient cavitation number K, the relationship $(b - K_o)/(b - K) = L/L_o$ must hold. This last result can be written in the form

$$\frac{K}{K_o} = \frac{L_o}{L} + \frac{b}{K_o}\left(1 - \frac{L_o}{L}\right) \quad ;$$

subject to the condition that V_o, the free stream velocity, is very high. Just how high the velocity V_o must be is determined from more detailed calculations below. A plot of K/K_o versus L/L_o is given in Fig. 7 for values of b/K_o from 1.0 to 2.0.

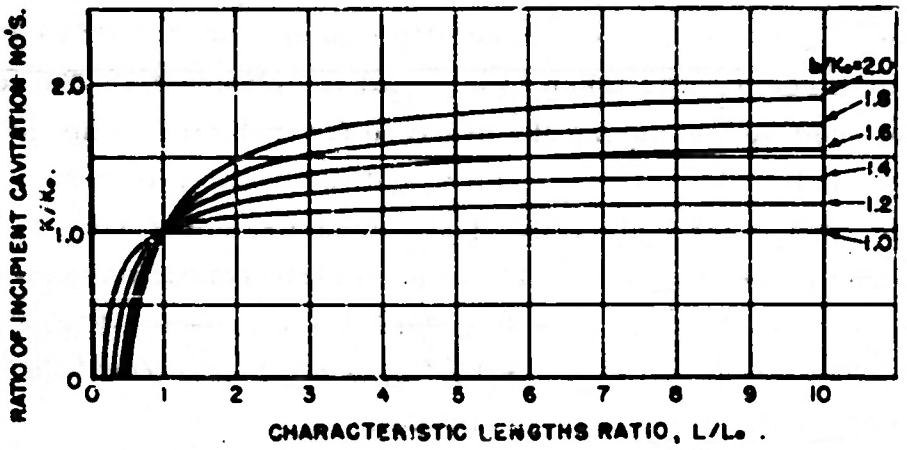

Fig. 7 - The scaling condition for incipient cavitation for very large free stream velocities ($V_o \longrightarrow \infty$)

Calculations for Incipient Cavitation on the Joukowski Hydrofoils

Calculations for incipient cavitation on the Joukowski hydrofoils will now be made by means of the procedures developed above. The relationships which must be used for the numerical work are

$$\sigma = \left(\frac{\frac{\pi}{4} + m - 1}{m}\right)^2 \frac{R_o \rho V_o^2}{4\sigma} (b - K) \quad ;$$

$$(m - 1) = \ell_2/\ell_1 \quad ;$$

$$\tau = \frac{2(\ell_1 + \ell_2)\sqrt{b - K}}{V_o\left(\sqrt{b} + (1 + b)\sin^{-1}\sqrt{\frac{b}{1+b}}\right)} \sqrt{\frac{2\sigma}{\rho R_o^3}} \quad ;$$

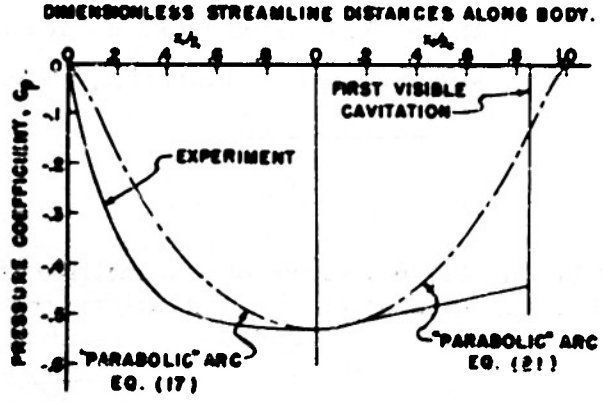

Fig. 8

and a graph of the function $\tau = F(\sigma, \gamma)$, Fig. 5. In order to find m, the experimental pressure distributions for the three Joukowsky hydrofoils were corrected for tunnel blockage (1), and a single curve was faired through the points, as shown in Fig. 8. It was observed experimentally that the first visible cavitation on the hydrofoils occurred at about 20% of the chord, c, from the point where the pressure

distribution C_p is first zero. In an effort to account for this experimental fact, the distance ℓ_2 was taken to be equal to $0.25c - \ell_1$. The length ℓ_1 was determined by measuring the distance from the minimum pressure point to that point where the pressure coefficient, C_p, is zero nearest to the leading edge of the hydrofoil. These measurements gave $\ell_2/\ell_1 = 14/11$ so that $(m - 1) = 1.27$. These geometric relationships and the approximating parabolic pressure distribution are shown in Fig. 8. If one takes $\sigma = 70$ dynes/cm, $R_o = 2 \times 10^{-4}$ cm, $\rho = 1$ gram/cm^3, $b = 0.53$, the equation for the dimensionless time is

$$\tau = 1.28 \times 10^6 \frac{c}{V_o} \sqrt{0.53 - K} \quad ,$$

and for the bubble-driving parameter,

$$\alpha = 0.581 \times 10^{-6} (0.53 - K) V_o^2 \quad .$$

By means of the graph for $\tau = F(\alpha, \gamma)$, with $\gamma = 1.0$*, trial and error calculations were made to find K for values of the free stream velocity V_o of from 900 cm/sec to 3000 cm/sec for each of the three chord lengths, 2 in. (5.08 cm), 4 in. and 8 in. The calculations were extended to infinite velocity by means of Eq. (45) (for this case C = 550 cm). For the case c = 4 in., the calculations were repeated for zero air content ($\gamma = 0$). From these calculations, curves of incipient cavitation number K versus the ratio c/V_o are given in Fig. 9. The calculated results are also compared with experiment in Fig. 9. The experimental scatter is too great to draw any definite conclusions as to the applicability of the theoretical results. The calculated curves show the tendency for the cavitation number to increase with velocity for all scales, and, except for the higher velocities, no scale effects are found at constant velocity. The data do not conclusively prove or disprove these theoretical findings.

---

*$\gamma = 1$ corresponds to an initial bubble air pressure of 700 millibars or a dissolved air concentration of 70%, the saturation concentration for an air pressure of 1 atmosphere above the water.

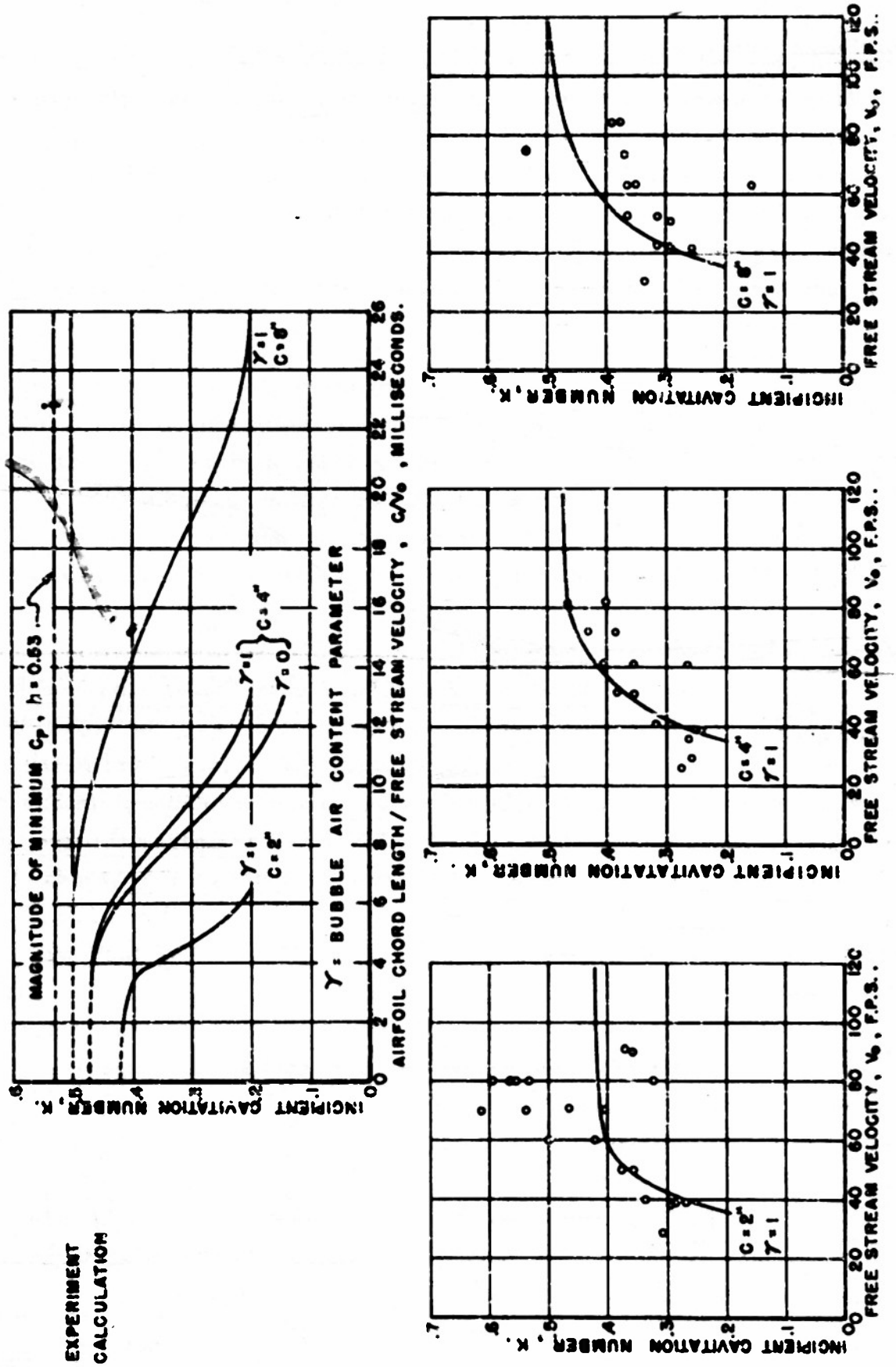

Fig. 9 - Calculated and experimental results for incipient cavitation on the Joukowski Hydrofoils

Calculations for Incipient Cavitation on the "Hemispheres"

Calculations were made for the inception of cavitation on right cylindrical bodies with hemispherical noses. The same body sizes were selected as were used by R. W. Kermeen in his experiments (see Ref. 1). Kermeen found that the dissolved air concentration in the water during his experiments was about one-half of the saturation value for an air pressure of one atmosphere. The corresponding value of the air content parameter, γ, was taken to be 0.7.

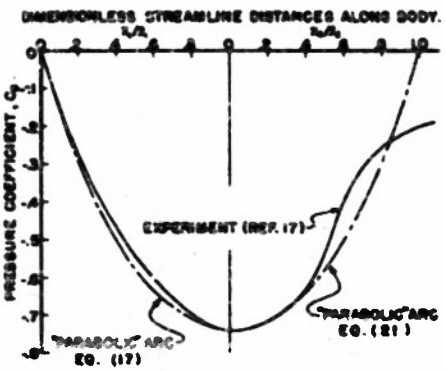

Fig. 10

The experiments of Rouse[9] show that b, the absolute value of the minimum pressure coefficient on the body, increases from about 0.65 at a Reynolds number of 0.6×10^5 to 0.74 when the Reynolds number is greater than or equal to 1.2×10^5. This change in the minimum pressure, b, was accounted for in the determinations of the dimensionless time, τ, (Eq. 23) and of the bubble-driving parameter, σ, (Eqs. 7 and 43). The "parabolic" pressure distribution was fitted to the experimental pressure distribution by selecting for the pressure distribution asymmetry factor, m, a value of 1.45. Figure 10 compares the experimental and the "parabolic" pressure distributions when the Reynolds number is in the supercritical regime ($R_e \geq 1.2 \times 10^5$). Trial and error calculations were then performed in the same fashion as for the Joukowski hydrofoils. The calculations are compared with Kermeen's data in Fig. 11. It will be seen that the calculated values of incipient cavitation number are in poor agreement with experiment. The disparity between the experimental and the calculated results increases as the size of the body decreases. There are two possible reasons for the disagreement. Either the mathematical approximations used in developing the theory are too great, or some physically important effect (such as that due to the boundary layer) has been overlooked. It may well be that both of these factors contribute to the large differences between theory and experiment.

It will be noticed in Fig. 11 that for the 2, 1-1/8 and 1/4 inch models the experimental data for incipient cavitation number seem to show little

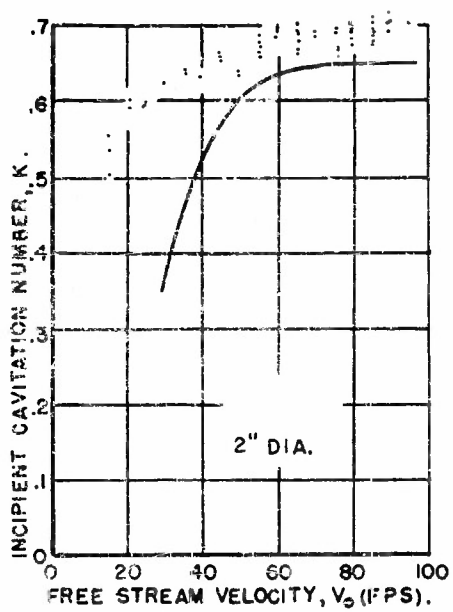

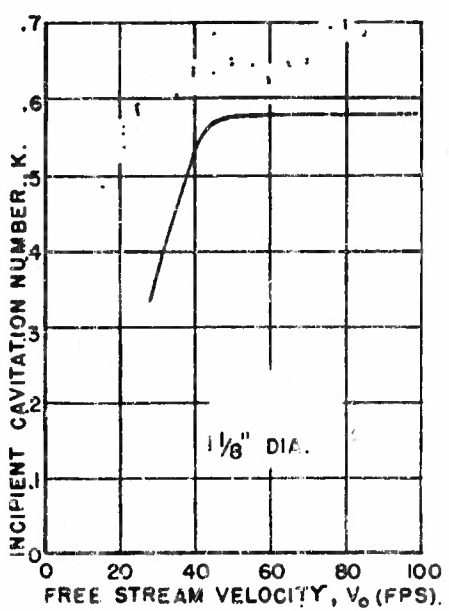

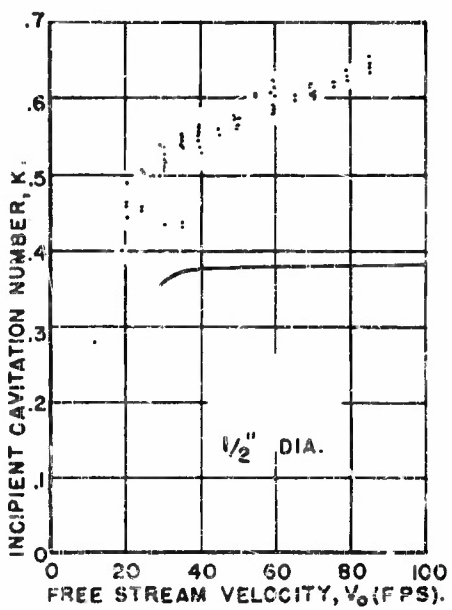

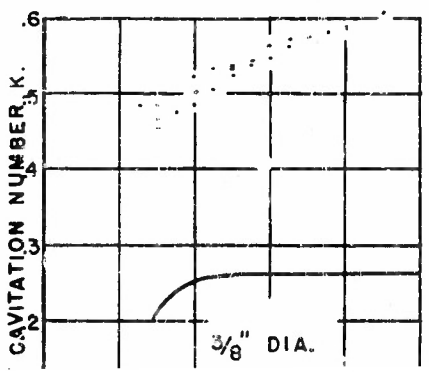

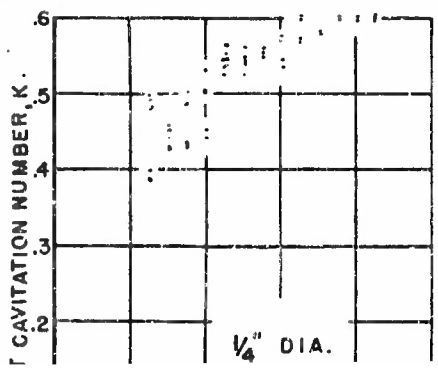

· EXPERIMENT, R.W. KERMEEN.

— CALCULATED.

or no dependence upon the free stream velocity, V_o, when V_o is greater than or equal to 80 ft per sec. This apparent independence of the incipient cavitation number with free stream velocity corresponds to the theoretical conditions leading to Eq. (46). Equation (46) relates the incipient cavitation number to the characteristic body length of similar bodies under the condition that the free stream velocity is very high. The incipient cavitation number under this condition is said to have attained its limiting value. If it is supposed that the experimental data, for the highest free stream velocities measured, approximate such limiting values of the incipient cavitation number, it is reasonable to compare the experimental points for this case with Eq. (46).

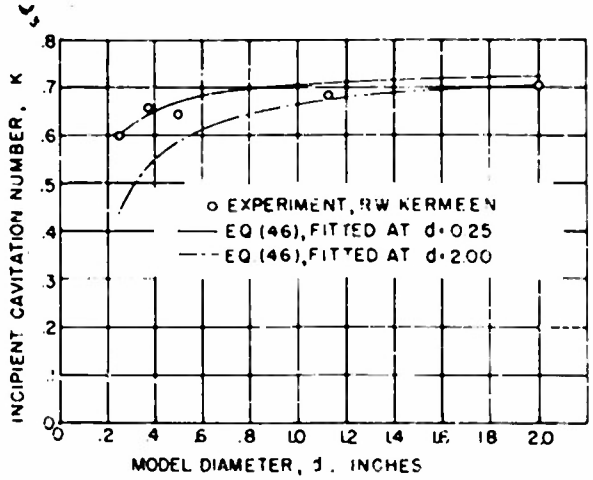

Fig. 12

The data for incipient cavitation number on each model at the highest test velocity were averaged and plotted against model diameter in Fig. 12. Equation (46) was then fitted to the experimental points twice at diameters of 1/4 in. and 2 in., respectively. The two curves are shown in Fig. 12. It will be seen that the agreement between experiment and theory is best when the calculations are fitted to the smallest model. The free stream velocity in all cases was at least 80 ft per sec. Perhaps data for even higher values of V_o would give better agreement when the theory is compared with experiment. More experiments must be made to test this point. The theoretical trends (Figs. 9 and 11) seem to indicate that the limiting value for the incipient cavitation number will be attained for higher velocities, V_o, for large bodies than for small models. If this trend is correct it means that most water tunnels cannot reach high enough speeds to make use of this theoretical approximation when models with low pressure regions larger than that of the two-inch diameter hemisphere are tested.

It will be recalled that in deriving Eq. (46), as with all other theoretical results, two basic approximations were made. First, the pressure was estimated from experimental results and Bernoulli's Law. Second, the time during which the nucleus is exposed to a low pressure condition

where bubble growth can occur was estimated from the body length and the liquid velocity along the body just outside the boundary layer. The application of Bernoulli's Law should give quite accurate results. One must conclude, therefore, that the time estimates are not good enough for the present purposes. Furthermore, if one traces through the calculation procedure for the inception of cavitation, he will find that underestimating the time results in an underestimate of the cavitation number for incipient cavitation. The present calculations do not account for the possibility that at least a portion of the bubble growth occurs in the boundary layer where the time available for growth would be greater than the time estimates used here. Thus, before one can make predictions for the inception of cavitation with confidence, the boundary layer's effect on growing cavitation bubbles must be understood.

PART III

CONCLUSIONS*

It is found by experiment that cavitation on submerged bodies in a rectilinear flow shows decided changes in its development as the free stream velocity and body size are changed. It is found that under certain conditions the incipient cavitation number depends on both body scale and free stream velocity. Of these two effects, that due to changes in free stream velocity is the greater, and most of the monotonic increase in incipient cavitation number with free stream velocity occurs below a free stream velocity of 60 fps. In the velocity range between 30 and 60 fps the cavitation number changes by about 25% of its maximum value. For velocities above 60 fps the incipient cavitation number increases by less than 10% of its maximum value. At constant velocity the incipient cavitation number increases with scale. However, more work must be done before truly quantitative results can be given for the scale effect at constant velocity.

It was found that one cannot obtain useful scaling laws for limited cavitation from similarity arguments. In fact, the similarity calculations show that one may expect limited cavitation to be affected by both body size and free stream velocity. One is then led to conclude that the cavitation number, K, is not the only significant parameter required to define the limited cavitation flow regime. Both experiment and analysis indicate that one must specify the model size, free stream velocity, dissolved air content and the cavitation number if he wishes to describe completely an experimental situation for an immersed body of specified shape. The condition of the body surface should also be specified, but this effect has not been considered in this paper. Although it is convenient to use the cavitation number, K, for theoretical calculations, one would be closer to the physical relationships if, instead of the cavitation parameter, he specified the liquid vapor pressure and the free stream static pressure.

From the lack of agreement between experiment and the greatly simplified theoretical calculations presented in this report, one can

---

*These conclusions summarize the results of both the preliminary report(1) and the work presented in this paper.

conclude that the neglect of the role of the boundary layer is not justified for precise predictions of the effects of model scale and free stream velocity upon the inception of cavitation. Further, the use of an arbitrary final radius instead of a specified maximum radius for the required bubble growth may have introduced an extraneous variability in the calculations. On the other hand, the qualitative agreement between the experimental and calculated trends for incipient cavitation number versus free stream velocity and body size, substantiates the basic premise that scale effects in limited cavitation arise because of transient pressure effects on the nuclei in the liquid flow.

A combination of simple theoretical considerations and some of the experimental data for incipient cavitation gives estimates for the effective initial nucleus radius. It is found that for the water used in the experiments, the calculated effective initial radius is between 10^{-4} and 10^{-3} centimeters.

For the limiting case where the free stream velocity approaches infinity, it is found that the cavitation number, K, for incipient cavitation does not approach b, the absolute value of the minimum pressure coefficient on the submerged body. Instead, the limiting value of the incipient cavitation number approaches a value less than b, and the difference, $b - K$, is found to be inversely proportional to the characteristic body length, L. The theory closely approximates the experimental results if the equation is fitted to the data for the smallest model. More experimental work is needed to demonstrate the complete validity of this result.

BIBLIOGRAPHY

1. Parkin, B. R., "Scale Effects in Cavitating Flow - A Preliminary Report", California Institute of Technology, Hydrodynamics Laboratory Report No. 21-7, December 1951.

2. Reichardt, H., Reports and Translations No. 776, Ministry of Aircraft Production (1946); distributed by Office of Naval Research, Navy Dept., Washington, D.C.

3. Kermeen, R. W., "Some Observations of Cavitation on Hemispherical Head Models", California Institute of Technology, Hydrodynamics Laboratory Report No. E 35.1, June 1952.

4. Eisenberg, P., "On the Mechanism and Prevention of Cavitation", David W. Taylor Model Basin Report No. 712 (1950).

5. Rattray, Maurice, Jr., "Perturbation Effects in Bubble Dynamics", California Institute of Technology, Hydrodynamics Laboratory Report No. 25-5, January 1951.

6. Epstein, P. S., and Plesset, M. S., "On the Stability of Gas Bubbles in Liquid-Gas Solutions", Jour. Chem. Phys., Vol. 18, No. 11, pp. 1505-1509, November 1950.

7. Epstein, P. S., "Textbook of Thermodynamics". John Wiley and Sons, Inc. (1937). Ch. IX, p. 159.

8. Plesset, M. S., "Rate of Formation of Vapor in a Uniformly Heated Liquid". North American Aviation, Inc., Special Research Report NAA-SR-53 (1949).

9. Rouse, Hunter, and McNown, J. S., "Cavitation and Pressure Distribution", and "Head Forms at Zero Angle of Yaw", State Univ. of Iowa, Studies in Engineering, Bulletin 32, p. 12, (1948).